

See discussions, stats, and author profiles for this publication at:
<https://www.researchgate.net/publication/244327981>

Configuration interaction study of the excited states of CO adsorbed on a Pt₉₇ cluster

ARTICLE in CHEMICAL PHYSICS · JUNE 2003

Impact Factor: 1.65 · DOI: 10.1016/S0301-0104(03)00188-5

CITATIONS

7

READS

17

5 AUTHORS, INCLUDING:



[R.J. Buenker](#)

Bergische Universität Wuppertal

168 PUBLICATIONS 1,934 CITATIONS

SEE PROFILE



[Heinz-Peter Liebermann](#)

Bergische Universität Wuppertal

136 PUBLICATIONS 1,282 CITATIONS

SEE PROFILE



[Ekaterina I Izgorodina](#)

Monash University (Australia)

67 PUBLICATIONS 2,528 CITATIONS

SEE PROFILE

Configuration interaction study of the excited states of CO adsorbed on a Pt₉₇ cluster

R.J. Buenker^{a,*}, H.P. Liebermann^a, D.B. Kokh^a, E.I. Izgorodina^a, J.L. Whitten^b

^a Fachbereich 9, Theoretische Chemie, University of Wuppertal, Gausstrasse 20, 42097 Wuppertal, Germany

^b Department of Chemistry, North Carolina State University, Raleigh, NC 27695-8204, USA

Received 8 November 2002; in final form 9 April 2003

Abstract

A procedure is developed to obtain pseudo-canonical localized molecular orbitals for use in *ab initio* multireference CI calculations of the electronic spectra of molecules adsorbed on the surfaces of large clusters of metal atoms. The Pt₉₇CO system is employed as a test and potential curves are computed for a large number of its electronic states. The present method is able to accurately describe internally excited states of the adsorbed CO molecule without computing most of the charge-transfer states of lower energy which occur in the same MRD-CI secular equations. It is found that the potentials of the $\sigma-\pi^*$ states are repulsive along the Pt–C coordinate and hence that their transition energies from the ground state are much higher (11.4–11.6 eV) than for the isolated CO molecule. The corresponding $\pi-\pi^*$ states are all relatively strongly bound, however, similarly as for the ground state, with transitions to them occurring as much as 1 eV lower than when the Pt₉₇ cluster is absent. This behavior can be traced to the fact that the Pt–C bonding orbital in the ground state has a large amount of CO sigma character, consistent with earlier calculations reported for the Pt₇CO model system, whereas neither the π nor the π^* MO is strongly affected by the approach of the metal cluster.

© 2003 Elsevier Science B.V. All rights reserved.

1. Introduction

The configuration interaction (CI) method is well-known to be a powerful tool for the calculation of excited states of small molecules. The size of the configuration space which needs to be considered explicitly in a given application depends factorially both on the number of active electrons of the system and on the number of

atomic orbitals (AOs) employed in the theoretical treatment. This feature does not prevent one from carrying out accurate calculations of the photochemistry of small molecules adsorbed on extended systems with this method, however. Whitten and Yang [1] have developed an embedding procedure for clusters of heavy atoms to simulate metal surfaces, for example, which allows one to treat the adsorbed molecule and one or more metal atoms at a higher theoretical level than the rest of the system. A localized molecular orbital (LMO) procedure can then be implemented for a CI treatment which produces orthonormal one-electron basis functions of two distinct types:

* Corresponding author. Fax: +49-2226-918568/202-439-2509.
E-mail address: buenker@uni-wuppertal.de (R.J. Buenker).

(a) those confined to the adsorption site, and (b) those representing the metal surface environment.

To deal with excited states, it is quite important to use LMOs which are still closely related to the canonical MOs of the system, that is, those which diagonalize the Fock operator of self-consistent field (SCF) theory, because the latter have proven to be quite suitable for describing spectroscopic transitions. It is therefore necessary to find a reliable procedure which prevents the canonical orbitals from being unnecessarily transformed among one another merely for the purpose of obtaining a strictly localized basis. Such a procedure will be described below and will be tested in a large-scale CI treatment for a meaningful example. The system chosen is Pt_{97}CO , which can be used to study the adsorption of carbon monoxide on a $\text{Pt}(111)$ surface. Previous calculations for a smaller model system, PtCO surrounded by a hexagon of Pt atoms, reported earlier [2] are available for comparison, whereby in that case it was possible to obtain useful results without the benefit of a localization procedure. It will be shown that the present method is capable of accurately representing both internal excited states of the CO adsorbate as well as those in which an electron is transferred from the metal surface to the attached molecule.

2. Description of the localization technique

The localization procedure employed in the present work is that of exchange maximization [3,4]. For this purpose, one needs a set of reference orbitals relative to which the exchange matrix in the AO basis employed is computed. It has been found to be critical to use atomic reference orbitals and not symmetrized linear combinations in this reference set. As a consequence it is not possible to take advantage of symmetry blocking in the ensuing CI treatment, which is normally quite helpful for small systems. In practice this represents a minor restriction in the present applications, however, because the metal cluster/adsorbate systems of interest are generally devoid of any global symmetry. In the present case, the cluster geometry for Pt_{97} , as shown in Fig. 1, does contain a plane of

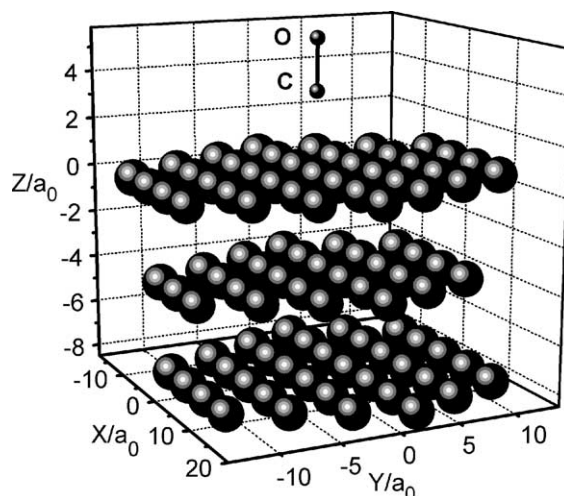


Fig. 1. Schematic diagram depicting the geometrical arrangement of the Pt_{97} cluster employed in the present study and its relation to the adsorbed CO molecule. The placement of the atoms is the same as for three layers of a (111) surface of platinum metal.

symmetry, however, and one is still able to take advantage of this fact in the CI calculations, as will be discussed in the next section.

The localization transformation must be carried out separately in the occupied and virtual SCF-MO spaces in order to preserve the total energy of the single-determinant wave function. In practice only closed-shell SCF states are considered for this purpose, whereby it is assumed that the CI treatment is capable of recovering any possible errors introduced by not using open-shell or multiconfigurational SCF MOs in a given case. As mentioned in Section 1, however, the resulting exchange-maximized occupied and virtual LMOs are not directly suitable for the calculation of excited states because one needs to be able to clearly identify initial and final MOs in the corresponding transitions, and that is best done with conventional MO theory, that is, with the canonical MOs for which Koopmans' theorem holds. To circumvent this difficulty, a partitioning method has been implemented which further divides the occupied and virtual LMOs into subsets based on the value of their exchange integrals with the reference AOs.

In the present case, for example, the Pt_{97}CO system has 68 electrons in the SCF treatment, 54 from the platinum cluster and 14 from CO. The

resulting 34 doubly occupied orbitals are divided into two partitions of 23 and 11 LMOs, characterized by the largest and smallest exchange integrals, respectively. Each set is used to form a matrix representation of the Fock operator obtained with the electronic field of the converged solution, and this is subsequently diagonalized in each case to obtain pseudo-canonical orbitals for use in the CI treatment. Since the reference orbitals are located on the CO molecule and the central Pt atom in this example, the corresponding inner-shell MOs are found in the first set, namely the two 1s orbitals of C and O and the 5s and 5p shells of Pt. The remaining 17 LMOs are placed in the active set for the CI calculations, while the latter six are combined with the other 11 occupied orbitals from the second partition to form the corresponding set of core orbitals, that is, those which are doubly occupied in all configurations. In general, it is necessary to experiment with the localization procedure to ensure that key occupied orbitals are included in the active space while holding the number of active electrons to a practical minimum which is consistent with the capabilities of the CI method.

The choice of virtual MOs is also a critical factor for the CI treatment. In the present case it is essential to have a good representation of the π^* orbital of CO, for example. This has been accomplished by dividing the virtual MOs into two sets, 29 of the most localized in one partition and the remaining 38 in the other. Since the π^* MO components are localized in the region from which the reference AOs are taken, it is expected that they will be found among the set of pseudo-canonical orbitals resulting from diagonalization of the Fock matrix corresponding to the more localized set. This procedure works quite effectively for Pt_{97}CO and results in π^* LMOs which are very similar to those which result from open-shell SCF calculations in which orbitals of this type are occupied. The orbital energy order of the π^* pseudo-canonical LMOs varies from one nuclear conformation to another, and so care has to be taken in identifying them for occupation in the various excited state configurations over the entire potential surface to ensure maximum continuity. Beyond this, one has the option of eliminating

some of the virtual orbitals from the CI treatment, and this has been done for the most compact C and O LMOs in the present case.

Provided the above localization procedure has been carried out in a manner which is consistent with the electronic structure of the system at hand, multireference single- and double-excitation (MRD-CI [5–8]) calculations can be carried out on the basis of the resulting LMOs. In the present case, the active orbital space consists of 82 LMOs and there are 34 active electrons in the CI. More generally, one expects to be able to treat as many as 50 active electrons with up to 200 active LMOs in the basis, and this allows one to obtain reliable predictions for a wide range of excited states which are necessary for the description of photochemical processes on metal surfaces. It is sometimes preferable to employ reference AOs which are located entirely outside the adsorption region. In this case the occupied LMOs with the largest exchange values are generally placed in the core of the CI calculations, while those with the smallest values are assigned to the active space. It is advisable to try both methods before settling on a final treatment, as well as to vary the sizes of the LMO partitions employed to obtain satisfactory representations of the key orbitals involved in the electronic transitions of interest in a given case.

3. Details of the CI calculations

The geometrical arrangement of the Pt_{97} cluster is chosen to simulate the $\text{Pt}(1\ 1\ 1)$ surface (Fig. 1). The Pt interatomic distances are fixed throughout the calculations. Core potentials are employed for each of the atoms, but with varying numbers of shells. The 5s, 5p and 5d electrons of the central atom to which CO is adsorbed are described by basis functions. For 18 atoms only a single electron is outside the core region, whereas for 41 others all shells are described with core potentials. Partial charges are employed to describe the valence region of each of the other atoms: 12 with 5/6 e, 15 with 1/3 e and 10 with 3/10 e. This is done to simulate the effects of an infinite lattice. A single s-type basis function is employed for each of the 55 Pt atoms with partial or unit electronic charges.

The central Pt atomic basis consists of 2s, 2p and 2d functions [9], whereby only the component lying parallel to the CO axis is included for the 6p subshell (16 functions in all). Finally, a [4s2p1d] basis is used for both the C and O atoms, the same as in the earlier Pt₇CO study [2]. Altogether, the present AO basis consists of 101 AOs.

In accordance with the procedure outlined in the previous section, a closed-shell SCF calculation is carried out at each nuclear geometry considered to obtain a canonical MO basis. The localization technique is then employed to obtain LMOs for the core and active spaces of the CI treatment. A set of reference configurations is chosen to represent the most important electronic states to be described in the MRD-CI treatment. A divide-and-conquer strategy has been adopted to obtain the best possible description of the many roots of interest in this application. First of all, it is possible to distinguish the various reference configurations on the basis of symmetry despite the fact that the calculations are carried out without the use of symmetry orbitals. It was found that the key internal excited states of the adsorbed CO molecule typically occur as the 14–17th roots in the order of increasing energy even when the C_s symmetry of the system is taken into account, however. This is because of the many charge-transfer states which are also present in the spectrum of the combined cluster/adsorbate system. One can obtain some idea of the complexity of the calculations from the energy diagram of Fig. 2, in which potential curves for all ¹A' states up to and including the σ - π^* and π - π^* CO internal states of this symmetry are shown.

In order to obtain accurate results for each of these states, it was found to be preferable to treat them in groups of four to six states of each symmetry and multiplicity. To insure that the variation principle is satisfied to a satisfactory degree, some of these states were obtained in more than one CI secular equation, so that comparisons of corresponding energies and wave functions could be made in numerous cases. Typically six separate CI treatments were carried out for each of the four symmetry classes of states, and it was necessary to fine-tune the reference spaces to obtain suitably reliable results. This procedure relies on the fact

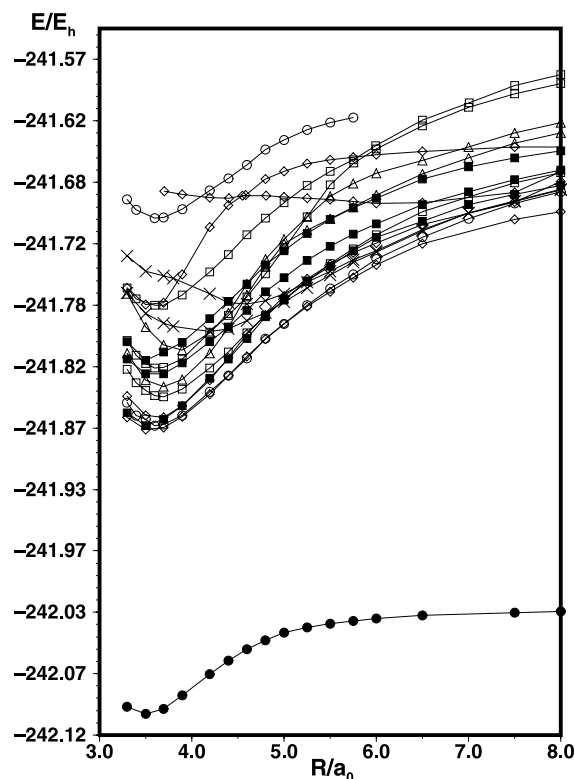


Fig. 2. Potential curves computed at the ab initio MRD-CI level of treatment for 17 ¹A' states of the Pt₉₇CO system along the Pt–C stretching coordinate. Note that most of the potential curves vary as 1/*R* toward large internuclear separations, indicating the charge-transfer character of the associated electronic states. Exceptions are for the ground state and the highest two excited states for small Pt–C values, which correspond to the ¹Δ and ¹Π internal CO states adsorbed on the Pt₉₇ cluster.

that in the LMO basis there are often only weak interactions between the dominant configurations of neighboring electronic states. It is the nature of metal cluster/adsorbate systems that this be so, and thus the present method takes advantage of a set of circumstances which otherwise produces a high degree of complexity in the electronic structure of such systems, namely the proliferation of low-lying states caused by the near degeneracies (continuum) in the bands of metal orbitals. It is clear that a similar approach would be largely ineffective for small molecules, starting with the localization procedure itself, but it works quite satisfactorily in the present application.

The reference configurations employed in the MRD-CI calculations which produce the CO internal states are listed in Table 1. A configuration selection threshold of $T = 2\mu E_h$ was used and the sizes of the generated and selected single- and double-excitation spaces with respect to these reference species are also given (see Table 2). In addition to the $\sigma-\pi^*$ and $\pi-\pi^*$ configurations, it was found necessary to consider the corresponding excitations from the central Pt atom's $6s\sigma$ and $5d\sigma$ orbitals into the CO π^* (and sometimes also s ring- π^* and $5d\pi-\pi^*$) in the same secular equation. The closed-shell ground state configuration was also included to allow for a comparison between the energy obtained for it in this case with that resulting from calculations designed specifically for this state in which the above excited configurations were excluded from the reference set. Inevitably, one has to use a lower standard for including configurations which make non-negligible contributions to the CI wave function of a given state because they may themselves be dominant configurations for other states. In this situation one must rely more heavily on approximations such as the multireference Davidson correction [10,11] which

account for the effects of higher-order excitations in the correlation treatment.

4. Calculated results

The computed CI potential curves for the Pt–C stretching vibration of various states of the Pt_{97}CO system are shown in Figs. 3(a)–(d). Corresponding relative energy values are given in Table 3. The ground state adsorption energy for CO on platinum is found to be 2.31 eV at the estimated full CI level, that is, when the generalized Davidson correction [10,11] is taken into account. This value is only 0.03 eV less than calculated for the analogous quantity for the Pt_7CO model system treated previously [2]. In that study the basis set superposition error (BSSE) was found to be 0.7 eV at the CI level, whereas it is 0.57 eV in the present treatment, the lower value reflecting the improved central Pt atom basis employed in this case. If one applies the latter correction, an adsorption energy of 1.74 eV is indicated, which compares well with the 1.5 eV value reported from thermal desorption experiments for CO on Pt(1 1 1) [12]. A density functional theory (DFT) value of 1.64 eV has been reported for the same quantity [13]. The optimal Pt–C distance is computed to be 1.86 Å, almost exactly the same as for the Pt_7CO system [2]. The experimentally determined Pt–C equilibrium separation for atop adsorption is 1.85 Å [14].

In the previous calculations for Pt_7CO it was only possible to obtain charge-transfer states at the large-scale CI level. Internally excited states of the CO adsorbate were computed at short Pt–C distances in quite small reference secular equations (4×4). The LMO technique described in Section 2 overcomes this deficiency in the present calculations with a much larger cluster of Pt atoms. Two of the CO internal state potential curves can be seen in Fig. 3a for the $^1A'$ states, for example. At short Pt–C distances the lowest two excited states shown are found to have primarily charge-transfer compositions, corresponding to excitations from the central Pt atom $5d\sigma$ and $6s\sigma$ orbitals into the π^* of CO. Their potentials have characteristic $1/R$ behavior as they approach infinite separation. They become fairly irregular in the Pt–C = 7.5–

Table 1

Reference configurations employed in the MRD-CI calculations for the Pt_{97}CO system. Four secular equations are solved for the $^1,^3A'$ and $^1,^3A''$ symmetry classes of electronic states at each nuclear geometry

Leading CO internal configurations	Charge transfer satellite configurations
Ground state (closed shell) ^a	Pt $6s\sigma-\pi^*$ ^b
$\sigma-\pi^*$	Pt $5d\sigma-\pi^*$
$\pi-\pi^*$	Pt $5d\pi \rightarrow \pi^*$ ^c
	Pt ring $s\pi \rightarrow \pi^*$ ^c

^a Only used for the $^1A'$ space.

^b Excluded in the 3.3–4.4 a_0 Pt–C range for the $^1A'$ space.

^c Only included in the 3.3–4.4 a_0 Pt–C range for the $^1A'$ space.

Table 2

Dimensions for the selected and generated CI spaces (Pt–C = 3.50 a_0 , $T = 2.0\mu E_h$)

Symmetry	Roots	SAF/sel.	SAF/total
$1A'$	5	56 013	6 522 305
$1A''$	4	49 240	6 236 159
$3A'$	5	74 023	10 884 627
$3A''$	5	73 995	10 884 627

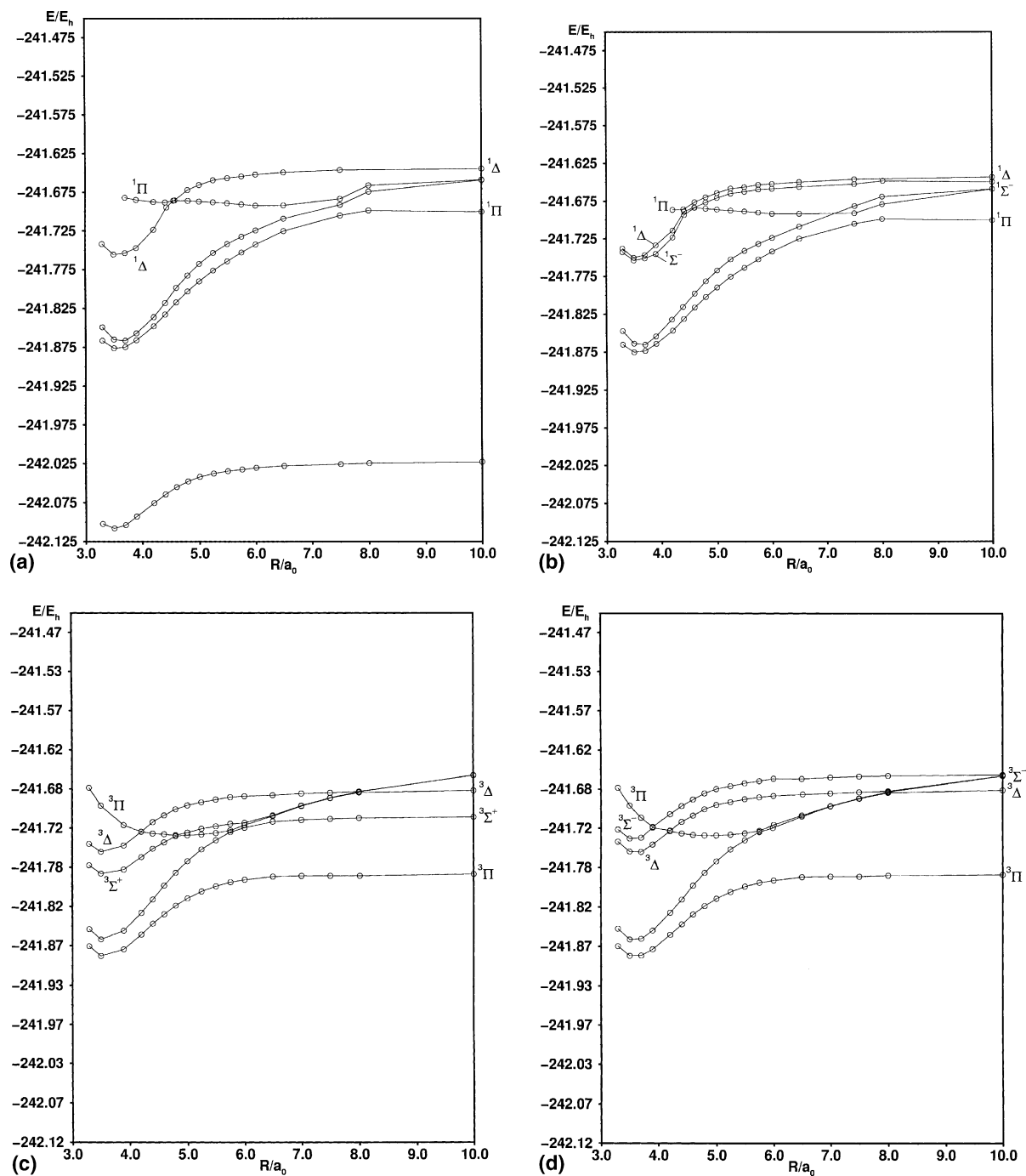


Fig. 3. Potential curves computed at the ab initio MRD-CI level of treatment along the Pt–C stretching coordinate for selected states of: (a) $1A'$, (b) $1A''$, (c) $3A'$ and (d) $3A''$ symmetry for the Pt_7CO system. The internally excited CO states are labeled in accord with their symmetry designations in the isolated molecule.

Table 3

Relative energies E (in eV) of various electronic states of the Pt_{97}CO system at two Pt–C internuclear distances ($3.5a_0$, close to the near equilibrium separation of the ground state, and $10.0a_0$). The results are given at the estimated full CI level of treatment. Adsorption energies, computed as the difference of these two values for each state, are also given. The corresponding relative energies obtained for states of the isolated CO molecule are also listed in parentheses for comparison with the results obtained for the cluster/adsorbate system at Pt–C = $10.0a_0$

Electronic state	E ($3.5a_0$)	E ($10.0a_0$)	Adsorption energy
Ground state ($^1A'$)	−2.31	0.00 (0.00)	2.31
$^1\Pi-A'$	9.27 ^a	8.77 (8.73)	(−0.50)
$^1\Pi-A''$	9.15 ^b	8.77 (8.73)	(−0.38)
$^1\Sigma^-$	7.32	10.14 (10.09)	2.82
$^1\Delta-A'$	7.27	10.28 (10.22)	3.01
$^1\Delta-A''$	7.42	10.32 (10.24)	2.90
$^3\Pi-A'$	8.88	6.50 (6.40)	(−2.38)
$^3\Pi-A''$	8.90	6.50 (6.40)	(−2.40)
$^3\Sigma^+$	6.52	8.48 (8.51)	1.96
$^3\Delta-A'$	7.28	9.39 (9.41)	2.11
$^3\Delta-A''$	7.31	9.43 (9.40)	2.12
$^3\Sigma^-$	7.75	9.96 (9.93)	2.21
Pt $6s\sigma-\pi^* ^1A'$	3.99	9.88	5.89
Pt $5d\sigma-\pi^* ^1A'$	4.30	9.89	5.59
Pt $6s\sigma-\pi^* ^1A''$	4.01	9.89	5.88
Pt $5d\sigma-\pi^* ^1A''$	4.33	9.88	5.55
Pt $6s\sigma-\pi^* ^3A'$	3.66	9.93	6.27
Pt $5d\sigma-\pi^* ^3A'$	4.24	9.92	5.68
Pt $6s\sigma-\pi^* ^3A''$	3.70	9.92	6.22
Pt $5d\sigma-\pi^* ^3A''$	4.27	9.93	5.66

^a Value at Pt–C = $3.70a_0$.

^b Value at Pt–C = $4.20a_0$.

$8.0a_0$ region, however, because of their intersection with the diabatic potential of the $\sigma-\pi^* ^1\Pi$ state, which becomes the lowest of the four excited states shown in Fig. 3(a) at large Pt–C values. Its potential remains nearly constant toward larger separations, identifying it clearly as a CO internal state, in contrast to the two potential curves immediately above it in this range. The vertical excitation energy of the $^1\Pi$ state at large Pt–C is 8.77 eV (based on the results at $10.0a_0$), which is in good agreement with the corresponding result for isolated CO employing the same AO basis (8.73 eV). In a full CI these two values would be exactly equal, and so this close agreement supports the conclusion that the MRD-CI treatment achieves a high degree of convergence toward this limit. The experimental adiabatic (T_0) excitation energy is only 8.07 eV [15], but there is a large relaxation effect due to the fact that the CO equilibrium bond distance is $0.20a_0$ greater in the $^1\Pi$ excited state than in the corresponding ground state.

It can be seen from Fig. 3(a) that the $^1\Pi$ internal state possesses a weakly repulsive Pt–C potential curve, first crossing the two charge-transfer states and then continuing upward. At Pt–C = $3.7a_0$ its energy is 0.50 eV higher than at the dissociation limit (see Table 3). This behavior is expected from the fact that the CO σ MO mixes with the highest energy Pt σ MO to form the relatively strong bond to the cluster in the corresponding ground state. Depopulating this orbital in the $^1\Pi$ excited state produces a net loss in binding energy of $2.31 + 0.50 = 2.81$ eV. The A'' component of the $^1\Pi$ state is similarly repulsive, lying 0.03 eV higher at Pt–C = $4.2a_0$. The CI coefficient for the $\sigma-\pi^*$ configuration remains quite large at this distance, with c^2 values of 0.81 and 0.83 computed for the A' and A'' $^1\Pi$ components, respectively. The computed vertical transition energies to these two states thus fall in the 11.4–11.6 eV range. These values are about 2 eV smaller than obtained previously in the earlier far less extensive CI treatment

for the corresponding states of Pt_7CO [2]. The conclusion remains, however, that the $\text{Pt}(111)$ surface has a strong effect on this transition, pushing it notably higher in the spectrum than is the case for isolated CO. Specifically, it does not appear on this basis that the UV/HREELS spectral features observed by Masel [16] in the 6–8 eV region can be the result of excitations into $\sigma-\pi^*$ internal CO states.

The situation is quite different for the $\pi-\pi^*$ transitions of CO, however. There are three singlet excited states with this configuration, as can be seen from Table 3. The lowest has $^1\Sigma^-$ symmetry and appears as a $^1A''$ state in the presence of the Pt cluster. The next of these states has $^1\Delta$ symmetry and thus has both an A' and an A'' component, while the $^1\Sigma^+$ state lies much higher in energy and becomes strongly perturbed by Rydberg states of the same symmetry. Potential curves have been obtained for each of these states except $^1\Sigma^+$, and they are found to have relatively deep minima in all cases. This behavior is expected because neither the π nor π^* MO is strongly involved in bond formation between CO and the Pt cluster, and so the adsorption energy for these states should be comparable to that of the ground state. The optimal Pt–C distance is also nearly the same for each of these excited states as for the ground state (see Figs. 3(a)–(d)). Some additional difficulties were encountered for these states because it was found that the charge-transfer configurations with which they most strongly interact differ for large and small internuclear separations. Suitably continuous potential curves were obtained by using a different set of satellite reference configurations for $\text{Pt}-\text{C} \leq 4.4a_0$ (see Table 1).

At large Pt–C the vertical excitation energies to $^1\Sigma^-$ and $^1\Delta$ are 10.14 and 10.28/10.32 eV, respectively, which again compare well with the corresponding values obtained for the isolated system of 10.09 and 10.23 eV. At $\text{Pt}-\text{C} = 3.5a_0$ the vertical energies are 9.63 and 9.58/9.73 eV, 0.5–0.7 eV lower. As one would suspect, the corresponding wave functions also remain nearly the same over the entire range of Pt–C distance considered. The two components of the $^1\Delta$ state also remain nearly degenerate throughout. The C–O bond distance for these states is $0.5a_0$ larger [15] than for the

ground state, so one expects the adiabatic transition energies to be considerably smaller than the above values and a relatively broad spectrum to be found in this energy region. In contrast to the $\sigma-\pi^*$ transitions, however, the perturbations caused by the presence of platinum are expected to be relatively small for the $\pi-\pi^*$ portion of the spectrum on the basis of the present calculations.

The corresponding potential curves for the triplet states of the Pt_7CO system are shown in Figs. 3(c) and (d). The analogous reference set of configurations is employed as for the singlet states discussed above (Table 1). At short Pt–C distances the lowest states shown are again of charge-transfer type. The lowest potential curve undergoes a much more strongly avoided crossing with the $\sigma-\pi^*$ state than is the case for the corresponding singlet states in Figs. 3(a) and (b). The $^3\Pi$ of the isolated CO molecule lies 6.40 eV above the ground state according to the present calculations (Table 3), 2.33 eV lower than $^1\Pi$, whereas the singlet–triplet splittings for the Pt d σ - and $\sigma-\pi^*$ -states lie only in the 0.1–0.3 eV range at short Pt–C separations. As a result, the $^3\Pi$ diabatic potential curve crosses that of the lowest charge-transfer state of the same multiplicity at a much shorter distance (ca. $5.5a_0$) in Figs. 3(c) and (d) than is the case for the corresponding singlets. The c^2 contribution of the $\sigma-\pi^*$ state varies rather slowly for the lowest (adiabatic) triplet wave function, as one expects for such a strongly avoided crossing. At $\text{Pt}-\text{C} = 3.7a_0$ the triplet–singlet splitting for the CO $\sigma-\pi^*$ A' states is only 0.39 eV. The key exchange integral responsible for this energy difference decreases considerably toward short Pt–C separations because the σ orbital is much more delocalized in this region than is the corresponding MO of isolated CO. The main consequence of this effect is that the $^3\Pi$ diabatic potential is significantly more repulsive than that of the corresponding CO $\sigma-\pi^*$ $^1\Pi$.

There are three $\pi-\pi^*$ triplet states of isolated CO (Table 3). The lowest-energy state is $^3\Sigma^+$ with a calculated vertical excitation energy of 8.51 eV. The other two have $^3\Delta$ (9.41 eV) and $^3\Sigma^-$ symmetry (9.93 eV). All three of the latter excitation energies agree within 0.05 eV of the corresponding values obtained from calculations for the Pt_7CO

system at $\text{Pt-C} = 10.0a_0$. In Figs. 3(c) and (d) the potential curves for these states are easily recognized because they all run parallel to the Pt–C axis at large distances. The $^3\Sigma^+$ state has an avoided crossing with the two charge-transfer states obtained in the present CI treatment in the neighborhood of $6.0a_0$. The latter potential curves continue upward toward large Pt–C where they exhibit the characteristic $1/R$ behavior. The $^3\Delta\text{--}A'$ has a similar crossing at larger Pt–C (Fig. 3(c)), but its potential curve runs very nearly parallel to that of $^3\Sigma^+$, with each reaching a minimum at nearly the same Pt–C value as the ground state. The computed adsorption energies are somewhat smaller than for the latter, however, namely 1.96 eV for $^3\Sigma^+$ and 2.11 eV for $^3\Delta\text{--}A'$, as compared to the 2.31 eV value for the ground state (results without the BSSE correction). Note that the corresponding values for the singlet $\pi\text{--}\pi^*$ states are 0.8 eV larger on the average because the pertinent exchange integrals decrease significantly as the Pt–C bond distance is decreased. The charge-transfer states also have a potential minimum in the same region, similarly as for the corresponding singlet states.

The $^3\Delta\text{--}A''$ potential curve is almost identical to that of its A' counterpart, so the degeneracy of the isolated CO state is practically unaffected by the presence of the Pt cluster. The $^3\Sigma^-$ state has a slightly larger binding energy (2.21 eV) than $^3\Delta$ (see Fig. 3(d)), but the difference is within the expected accuracy limits of the CI treatment (0.1–0.2 eV). In general, the indication is that the splittings between the three triplet $\pi\text{--}\pi^*$ states decrease with Pt–C distance but that each of their binding energies is still slightly smaller than for the ground state. For example, the vertical transition energy at $\text{Pt-C} = 3.5a_0$ for the $^3\Sigma^-$ state is computed to be 10.06 eV, whereas it is 9.96 eV at the dissociation limit. Each of their potential curves crosses that of $^3\Pi$ before attaining a minimum, but this occurs at a shorter Pt–C value than for the corresponding singlet states.

5. Conclusion

The localization method described above produces orbitals which are suitably canonical to al-

low for an accurate representation of the CO spectrum in the presence of an extended Pt cluster of atoms. Even though the internally excited states of CO lie far above numerous charge-transfer states, it is nonetheless possible to obtain Pt–C potential curves for them over a large range of internuclear distance. This is accomplished by restricting the corresponding reference configuration space so that only charge-transfer species which interact strongly with the internal CO configurations are included, which class in turn is minimized through the use of localized MOs.

It is found that the lowest-energy excited states of CO, which are of $\sigma\text{--}\pi^*$ type, have weakly repulsive Pt–C potential curves. This is understandable because the corresponding σ MO is quite important for the bonding of the ground state in the presence of the Pt cluster. The higher-energy $\pi\text{--}\pi^*$ states of the isolated molecule are much less affected by the approach of the Pt cluster, however, and so they become the most stable states in the CO spectrum in this environment.

Acknowledgements

The financial support of the Deutsche Forschungsgemeinschaft (BU 450/15-1), the US Department of Energy and the Fonds der Chemischen Industrie are hereby gratefully acknowledged.

References

- [1] J.L. Whitten, H. Yang, *Surf. Sci. Rep.* 24 (1996) 55.
- [2] R.J. Buenker, H.-P. Liebermann, J.L. Whitten, *Chem. Phys.* 265 (2001) 1.
- [3] J.L. Whitten, H. Yang, *Int. J. Quantum Chem. Symp.* 29 (1995) 417.
- [4] C. Edmiston, K. Ruedenberg, in: P.-O. Löwdin (Ed.), *Quantum Theory of Atoms, Molecules, and the Solid States*, Academic Press, New York, 1966.
- [5] R.J. Buenker, S.D. Peyerimhoff, *Theor. Chim. Acta* 35 (1974) 33, 39 (1975) 217.
- [6] R.J. Buenker, R.A. Phillips, *J. Mol. Struct. (Theochem)* 123 (1985) 291.
- [7] S. Krebs, R.J. Buenker, *J. Chem. Phys.* 103 (1995) 5613.
- [8] R.J. Buenker, S. Krebs, in: K. Hirao (Ed.), *Recent Advances in Multireference Methods*, World Scientific, Singapore, 1999, p. 1.

- [9] J.L. Whitten, H. Yang, Theoretical studies of ethyl to ethylene conversion on nickel to platinum, *Transition State Modeling for Catalysis*, American Chemical Society, Washington, 1999.
- [10] E.R. Davidson, in: R. Daudel, B. Pullman (Eds.), *The World of Quantum Chemistry*, Reidel, Dordrecht, 1974, p. 17.
- [11] G. Hirsch, P.J. Bruna, S.D. Peyerimhoff, R.J. Buenker, *Chem. Phys. Lett.* 52 (1977) 442.
- [12] H. Steininger, S. Lehwald, H. Ibach, *Surf. Sci.* 123 (1982) 264.
- [13] Y. Morikawa, J.J. Mortensen, B. Hammer, J.K. Nørskov, *Surf. Sci.* 386 (1997) 67.
- [14] D.F. Ogletree, M.A. VanHove, G.A. Somorjai, *Surf. Sci.* 173 (1986) 351.
- [15] K.P. Huber, G. Herzberg, in: *Molecular Spectra and Molecular Structure*, vol. 4 (Constants of Diatomic Molecules), Van Nostrand Reinhold, Princeton, NJ, 1979.
- [16] R.I. Masel, private communication.